# EXCITED STATE IN EVEN-EVEN FISSION PRODUCTS [*]

E. Cheifetz[†], R. C. Jared, S. G. Thompson, and J. B. Wilhelmy,

Lawrence Radiation Laboratory,
University of California,
Berkeley, California 94720, USA.

## ABSTRACT

Experimental results are presented on the ground state bands of 31 even-even nuclei produced in the primary fission of $^{252}$Cf. Systematics of the energies and life times of the transitions are given. From these data there is evidence indicating that a region of deformation in the $A \approx 100$ region may exist.

## 1. INTRODUCTION

In this talk we shall present information concerning the energy levels of very neutron rich even-even isotopes of elements with $38 \leqslant Z \leqslant 62$. Fission fragments from spontaneous fission of $^{252}$Cf provided experimental access to this region. The data which in a few of the cases can be correlated with already known levels, extend the knowledge about the systematic behaviour of collective excitations to neutron rich nuclei far from the beta stability line. The data include the lowest $2^+$ states (and in many of the cases some of the higher $4^+$, $6^+$ and $8^+$ levels) of all the isotopes that have calculated independent fission yield of more than 1% (with the exception of $^{136}$Te). This is shown in Figs. 1 and 2 where we present a modified chart of nuclides indicating the isotopes observed in this experiment. The systematics of the energy levels of

isotopes that are removed from closed shells are well fitted using the phenomenological model of Mariscoti et al.[1] There is evidence from level spacings and B(E2) values that light fission fragments such as $^{102}$Zr and $^{106}$Mo have rotational like behaviour. These results support recent theoretical studies of Ragnarsson and Nilsson[2] and Arseniev et al.[3] which have predicted a new region of stable deformation which includes these nuclei. Another feature of the results is the evidence that the well known abrupt discontinuity of the ratio $E4^+/E2^+$ for isotopes with 88 to 90 neutrons reaches its maximum effect in Nd, Sm and Gd, and becomes much smoother in the Ce and Ba nuclei.

## 2. THE EXPERIMENTAL TECHNIQUE

Prompt K x-rays and/or $\gamma$-rays in coincidence with pairs of fission fragments were measured using the detector arrangement indicated in Fig. 3. Three separate experiments using different photon detectors were performed: 1) recording $\gamma$-rays with a 1 cm$^3$ Ge(Li) detector (resolution 1 keV at 122 keV) in position $\gamma$2; 2) recording $\gamma$-rays and/or x-rays in coincidence using a 6 cm$^3$ Ge(Li) detector in position $\gamma$1 and a 2 cm$^2$ Si(Li) detector in position $\gamma$2; 3) recording $\gamma$-ray, $\gamma$-ray coincidences with a 35 cm$^3$ Ge(Li) coaxial detector in position $\gamma$2 and a 6 cm$^3$ Ge(Li) detector in position $\gamma$1. In all the experiments a nominally $10^5$ fission per minute source of $^{252}$Cf was electrodeposited onto the surface of fragment detector F1. Thus Doppler shifting and broadening problems were minimized for transitions from the fragments stopped in that detector. This technique, which simplified the spectra, applies to half life times longer than the stopping time of the fragments ($\sim 10^{-12}$ sec). Life time determinations in the time region 0.1 - 2.0 nsec were obtained from the

ratio of the non-Doppler shifted gamma ray intensity observed when the fragment stopped in the plated detector Fl relative to the intensity observed when the fragment stopped in the second detector F2, which was separated from the plated detector by 8 mm. The various detector systems were digitally gain stabilized using external gamma ray sources as indicated in Fig. 3

In all the experiments the analog pulse heights were digitized and stored event by event in a PDP-9 computer. The on-line computer was programmed to monitor the resolution of the detectors and to transfer the experimental data onto magnetic tape in a compressed format. A total $2 \times 10^{8}$ multiparameter events were recorded and later processed on a CDC 6600 computer.

The masses of the fragments were calculated from the measured energies using the Schmitt calibration method and the known neutron corrections[4]. Gamma-ray spectra associated with fragment masses in 2 amu wide mass intervals were obtained by sorting the three parameter data.

In Fig. 4 examples of high resolution $\gamma$-ray spectra associated with 2 amu mass intervals are shown. Each of these $\gamma$-ray spectra was then analyzed to give quantitative energies and intensities of individual transitions. This was accomplished using the on-line photopeak analysis code developed by Routti and Prussin[5]. The widths of the mass distributions associated with single gamma transitions ranged from 4.0 to 6.5 amu (FWHM) and the mean values of the masses for these distributions were determined with standard statistical errors of less than 0.2 amu for the strong transitions; however, the absolute determination of the masses are uncertain by ± 1 amu. This can be attributed mainly to the use of the average neutron corrections. The average value for a given mass is presumably too small for isotopes that are on the neutron

deficient side of the most probable isotope for a given element and conversely too large for isotopes on the neutron excess side. In some cases we have observed odd mass isotopes of even Z elements with experimental masses between those of the adjacent even isotopes although the latter were separated by less than 2 amu. There may also be a small smooth systematic error due to the uncertainties in the fragment pulse height to energy calibration procedure. The x-ray, gamma-ray coincidence data were used to obtain information on additional transitions associated with single isotopes.

3. RESULTS

The results of this investigation are summarized in Table I. For each isotope in the table we present the transition energies that were observed, the half life of the $2^+$ level and the yield per fission of the $2^+$ level (corrected for internal conversion). The considerations and criteria that have been used in assigning these levels have already been explained in two previous papers[6,7]. Some of the levels have been assigned by other workers and are repeated here because the transitions have been observed in the prompt gamma spectra. The cases in which our results have been correlated with other works are explained in the comments under the table.

Some of the lowest $2^+ \rightarrow 0^+$ transitions in isotopes on the neutron deficient side of the Zp line have been observed in (t,p) reactions and in post beta decay of fission products. Our results are in good agreement with values obtained by these other methods. This agreement confirms the techniques we have utilized for making level assignments.

Most of the transitions that we have assigned as $2^+ \rightarrow 0^+$ have also

been observed (though not previously assigned) in studies of gamma rays emitted following beta decay of unseparated prompt fission products.[10] These $2^+ \rightarrow 0^+$ transitions occurring after beta decay are observed with intensities which are substantial fractions of the cumulative mass chain yields. These measurements help substantiate that we are in fact observing ground state band transitions in the de-excitation of the prompt products.

## 4. DISCUSSION

### 4.1 Systematics of Energy Levels

The systematics of the energy levels of the ground state band in the cases where $E4^+/E2^+ \geqslant 2.3$ are well fitted using the phenomenological variable moment of inertia model of Mariscott et al.[1]. The results of $E6^+/E2^+$ and $E8^+/E2^+$ vs. $E4^+/E2^+$ for the ground state bands are shown in Fig. 5 which includes our current data and all the previously known experimental data that were summarized in reference 1. Although our data contains lighter nuclei than those of reference 1, no large deviations from the known systematic behaviour are observed.

The energies of the $2^+$ states obey smooth systematics. The trend shows a decrease in the $2^+$ level energies with **increased displacement** from the $N=50$ and $N=82$ shells. In the light fragments ($Z \leqslant 48$) there is a decrease of $2^+$ level energies with displacement from the $Z=50$ shell. On the other hand, in the heavy fragments ($Z \geqslant 50$) region isotopes with neutron number between 82 and 86 have an increasing $2^+$ level energies with increasing displacement from the $Z=50$ shell.

### 4.2 Rotational-like Light Fission Fragments

In Fig. 6 we present the systematic behaviour of the lowest $2^+$ levels and the $E4^+/E2^+$ ratio in the Zr-Pd region. One can see

clearly that the smooth decrease in level energies and corresponding smooth increase in the E4/E2 ratio in Pd becomes more rapid in Ru and Mo isotopes and then turns out to be an extreme jump between $^{98}$Zr - $^{100}$Zr. A similar behaviour is seen in Fig. 7 that shows the $B(E2)_{exp}/B(E2)_{single\ particle}$ ratio for this region. The B(E2) values were obtained from the measured energies and life time values following the formalism of Stelson and Grodzins.[17] The $\beta_2$ values in that formalism are $\sim$ 0.35 for $^{110}$Ru, 0.45 for $^{104}$Mo and $^{106}$Mo, and 0.6 for $^{102}$Zr. In principle, our reported life time values are upper limits because a hold up can occur in a transition before the $2^+ \to 0^+$ stage. This implies that the experimental B(E2) and $\beta_2$ values can only be higher.

The central question from these studies is whether the theoretical predictions for deformation can be verified. It is not possible to determine the existence of static deformations from observed energy level spacings or from measurements of B(E2; 2 → 0). However, studies of such systematics are indicative of nuclear softness and therefore it is of interest to compare these properties in this new region with the corresponding values for the rare earth and actinide regions which are the two major areas of known permanent deformation. There are several different indicators of deformation and it is informative to compare each. Figure 8 is a composite plot containing five indicators associated with deformation

$[\beta_2,\ B(E2)/B(E2)_{SP},\ E_4+/E_2+,\ \beta_2/\beta_{2SP},\ (79.51/E_2+) \times (158/A)^{5/3}]$ plotted as

a function of mass. The last indicator represents to a first approximation a mass independent comparison of the energies of the first $2^+$ states using arbitrarily the deformed $^{158}$Gd nucleus as a reference. The nuclei presented in the plot include the current, light fission product region, and a representative sampling of isotopes in the rare earths (150 - 180) and in the actinides (224 - 244).

In this light fission-product region, of the isotopes studied, $^{102}$Zr appears as the most favorable candidate for deformation. Its value for $\beta_2$ (0.604) and for the mass independent energy parameter (1.08) are larger than any of the corresponding values found in the rare earth and actinide nuclei. Also its values for $B(E2)/B(E2)_{SP}$ (234.) and $\beta_2/\beta_{2SP}$ (15.2) are larger than for any of the rare earths though smaller than some of the actinides. The only parameter for which it has a lower value than obtained in the other regions is the $E_{4+}/E_{2+}$ ratio where the $^{102}$Zr value of 3.15 is somewhat smaller than the limiting value for a perfect rotor (3.33) which is closely approached in both the rare earth and actinides. The other new isotopes for which we present information have smaller values for these deformation indicators than $^{102}$Zr but even they have, in several instances, values comparable or larger than those typically found in the rare earth and actinide region and in all cases are larger than the values found for spherical nuclei near closed shells.

For the isotopes with higher masses the decrease in the deformation indicators is believed to be due to the approach of the Z = 50 closed shell, and for the lighter isotopes the effect of the N = 50 shell should be important. The theoretical calculations of Arseniev et al.[3] imply that the regions of strongest deformation should be in the heavier isotopes of strontium (98 - 102) and of krypton (96 - 102) which are not produced in significant yield in the $^{252}$Cf fission process. The change in the energy of the lowest $2^+$ level between $^{98}$Zr and $^{100}$Zr is very extreme and larger than the well noted discontinuity between $^{150}$Sm and $^{152}$Sm. The 1.233 MeV first excited $2^+$ level in $^{98}$Zr is supported by recent $^{96}$Zr(t,p)$^{98}$Zr reaction studies[9] and also by our gamma ray spectra for which no line was found that could be attributed to a lower $2^+$ state.

For this $A \approx 100$ region the theoretically predicted[2,3] trend of increasing $\beta_2$ deformation with displacement from the Z = 50 shell was indeed found by the experiment, however the magnitude of the experimental $\beta_2$ value are much larger than the predicted values. This poses questions regarding the parameters of the Nilsson levels in this region and regarding dependence of the surface energy coefficient on the neutron excess. The very sharp changes in deformation parameters in the Zr isotopes are also not predicted by the calculations.

Although experimental information concerning rotational bands in neutron rich Ru nuclei has been reported previously by Johansson[18] and by Zicha et al.[19] we are unable to reproduce their results. We have not been able to find any of the γ-rays reported by them in coincidence with transitions we have assigned to the ground state bands of $^{108}$Ru and $^{110}$Ru.

### 4.3  88-90 Neutron Discontinuity

The data described here include Z = 56 and Z = 58 nuclei having 88 and 90 neutrons. The data show that the 88-90 neutron discontinuity is smearing out as the proton number decreases below Z = 60. This is seen both for the energies of the $2^+$ level and the $E4^+/E2^+$ ratio. A plot of the E4/E2 ratio of nuclei with $56 \leqslant Z \leqslant 70$ is presented in Fig. 9. This figure clearly shows that the maximum effect of the 88-90 neutron discontinuity occurs in the region $60 \leqslant Z \leqslant 66$. The nuclei with N = 92, Z = 58, and N = 92, Z = 68 have E4/E2 ratios and B(E2) values which indicate that they are as rotational as $^{152}_{62}$Sm, which is known to have permanent quadrupole deformation, even though for Z = 58 and Z = 68 the 88-90 neutron effect is relatively rather smooth. A similar effect has been shown to occur in the 76-80 proton number region[20] where a sharp discontinuity occurs for $106 \leqslant N \leqslant 112$ and a smooth behaviour was observed outside this region. We can summarize then that the transition from a vibrational spectrum to a rotational one

can be either abrupt or smooth depending probably on a delicate balance between proton and neutron pairing correlations. Calculations by Nilsson et al.[21] indicate that deformation is expected to occur abruptly between 86 and 88 neutrons for the nuclei discussed here. These calculations are similar to the ones described in the light fragment region. They are based on the Nilsson model combined with the Strutinsky normalization procedure and reproduce the general trend of decreased deformation for nuclei with 88 neutrons on both sides of Z = 62.

# REFERENCES

1. M. A. J. Mariscoti, Gertrude Scharff-Goldhaber, and B. Buck, Phys. Rev. <u>178</u>, 1864 (1969).

2. I. Ragnarsson and S. G. Nilsson, Lund Institute at Technology, Lund 7, Sweden, private communication (1969).

3. D. A. Arseniev, A. Zobieczewski, and V. G. Soloviev, Nucl. Phys. <u>A139</u>, 269 (1969).

4. R. L. Watson, J. B. Wilhelmy, R. C. Jared, C. Rugge, H. R. Bowman, S. G. Thompson, and J. O. Rasmussen, Nucl. Phys. <u>A141</u>, 449 (1970).

5. J. T. Routti and S. G. Prussin, Nucl. Instr. Methods <u>72</u>, 125 (1969).

6. E. Cheifetz, R. C. Jared, S. G. Thompson, and J. B. Wilhelmy, Phys. Rev. Letters <u>25</u>, 38 (1970).

7. J. B. Wilhelmy, S. G. Thompson, R. C. Jared, and E. Cheifetz, submitted to Phys. Rev. Letters and Lawrence Radiation Laboratory Report UCRL-19931, (1970).

8. R. Foucher, Orsay, France, private communication.

9. A. G. Blair, J. G. Beery, and E. R. Flynn, Phys. Rev. Letters <u>22</u>, 470 (1969).

10. R. F. Casten, E. R. Flynn, O. Hansen, T. Mulligan, R. K. Sheline, and P. Kienle, Phys. Letters <u>32B</u>, 45 (1970).

11. I. Bergström, S. Borg, P. Carle, G. Holm, and B. Rydberg, Annual Report 1969 Research Institute for Physics, Stockholm, p. 89 (unpublished).

12. W. John, F. W. Guy, and J. J. Weslowsky, submitted to Phys. Rev. and Lawrence Radiation Laboratory Report UCRL-72501 (unpublished).

13. T. Alväger, R. A. Naumann, R. F. Petry, G. Sidenius, and T. D. Thomas, Phys. Rev. <u>176</u>, 1105 (1968).

14. J. B. Wilhelmy, S. G. Thompson, J. O. Rasmussen, J. T. Routti, and J. E. Phillips, Lawrence Radiation Laboratory Report UCRL-19530, 1970, p. 178 (unpublished).

15. J. G. Bjerrgaard, O. Hansen, O. Nathan, and S. Hinds, Nucl. Phys. <u>86</u>, 145 (1966).

16. J. B. Wilhelmy, Lawrence Radiation Laboratory Report UCRL-18978, 1969 (unpublished).

17. P. H. Stelson and L. Grodzins, Nucl. Data <u>A1</u>, 211 (1965).

18. S. A. E. Johansson, Nucl. Phys. <u>64</u>, 147 (1965).

19. G. Zicha, K. E. G. Löbner, P. Maier-Komor, J. Maul, and P. Kienle, Intern. Conf. on Properties of Nuclear States, Montreal, August 25-30, 1969 (University of Montreal Press, 1969) p. 83.

20. J. Burde, R. M. Diamond, and F. S. Stephens, Nucl. Phys. A92, 306 (1967).

21. S. G. Nilsson, C. F. Tsang, A. Sobiczewski, Z. Symanski, S. Wycech, C. Gustafson, I. Lamm, P. Möller, and B. Nilsson, Nucl. Phys. <u>A131</u>, 1 (1969).

22. C. M. Lederer, J. M. Hollander, and I. Perlman, <u>Table of Isotopes</u>, 6th Ed., (John Wiley and Sons, Inc., New York, 1967).

23. F. S. Stephens, D. Ward, and J. O. Newton, Suppl. J. Phys. Soc. Japan <u>24</u>, 160 (1968).

Table I.  Experimental results for ground state bands.

| | Transition Energy in keV | | | | $t_{1/2}(2 \to 0)$ | Yield $2^+$ |
|---|---|---|---|---|---|---|
| | $2^+ \to 0^+$ | $4^+ \to 2^+$ | $6^+ \to 4^+$ | $8^+ \to 6^+$ | nsec | %/fiss. |
| $^{94}$Sr[a] | 837.4 | | | | | 0.51 |
| $^{96}$Sr[a] | 815.5 | | | | | 0.3⟩ |
| $^{98}$Zr[b] | 1223 | | | | | ∿ 0.⟨ |
| $^{100}$Zr | 212.7 | 352.1 | 497.9 | | 0.52 | 1 ⟩ |
| $^{102}$Zr | 151.9 | 326.6 | 486 | (587) | 0.86 | 1 ⟨3 |
| $^{102}$Mo | 296 | | | | | 0.⟨6 |
| $^{104}$Mo | 192.3 | 368.7 | 520.0 | | 0.45 | 3.37 |
| $^{106}$Mo | 171.7 | 350.8 | (511.8) | | 0.75 | 3.37 |
| $^{106}$Ru[c] | 269 | | | | | 0.16 |
| $^{108}$Ru | 242.3 | 423 | | | 0.22 | 1.44 |
| $^{110}$Ru | 240.8 | 423.1 | 576.1 | (707.7) | 0.23 | 3.49 |
| $^{112}$Ru | 236.8 | 408.9 | | | 0.20 | 0.97 |
| $^{112}$Pd | 348.8 | 535.8 | | | | 0.77 |
| $^{114}$Pd | 332.9 | 520.7 | 649.3 | | | 1.48 |
| $^{116}$Pd | 340.6 | 538.0 | | | | 0.87 |
| $^{118}$Cd | 488.0 | 677.3 | (805) | | | 0.32 |
| $^{132}$Te[d] | 974 | 990 | | | | ∿ 0.2 |
| $^{134}$Te,[d,e] | 1278 | 297 | 115 | | | 1.5 |
| $^{138}$Xe | 589.5 | 482 | | | | 2.3 |
| $^{140}$Xe | 376.8 | 457.9 | | | | 1.5 |
| $^{140}$Ba[f] | 602.2 | | | | | 0.52 |
| $^{142}$Ba[f] | 359.7 | 475.7 | 632 | | | 2.90 |

Table I. Continued

| | Transition Energy in keV | | | | $t_{1/2}(2 \to 0)$ | Yield $2^+$ |
|---|---|---|---|---|---|---|
| | $2^+ \to 0^+$ | $4^+ \to 2^+$ | $6^+ \to 4^+$ | $8^+ \to 6^+$ | nsec | %/fiss. |
| $^{144}$Ba | 199.4 | 530.4 | 431.7 | 510.8 | 0.49 | 3.60 |
| $^{146}$Ba | 181.0 | 333 | | | 0.85 | 1.01 |
| $^{144}$Ce$^g$ | 397.5 | | | | | 0.2 |
| $^{146}$Ce | 258.6 | 410.1 | 502.3 | | 0.29 | 1.04 |
| $^{148}$Ce | 158.7 | 295.7 | 386.5 | | 0.9 | 2.31 |
| $^{150}$Ce | 97.1 | 209 | 300.7 | 376.4 | > 0.9 | > 0.98 |
| $^{152}$Nd | 75.9 | 164.7 | 247.3 | 322.1 | > 2 | > 0.6 |
| $^{154}$Nd | 72.8 | 162.4 | 243.7 | 328.1 | > 2 | > 0.4 |
| $^{156}$Sm$^h$ | 76.0 | 174.2 | 268 | | > 2 | > 0.1 |
| $^{158}$Sm | 72.8 | 167.5 | 258.2 | 346 | > 2 | > 0.15 |

[a] The $2^+ \to 0^+$ transitions in $^{94}$Sr and $^{96}$Sr have been assigned by R. Foucher et al.[8] using an on-line mass separator.

[b] The first $2^+$ in $^{98}$Zr was found by Blair et al.[9] using the $^{96}$Zr(t,p)$^{98}$Zr reaction.

[c] The first $2^+$ in $^{106}$Ru was reported by Casten[10] and was produced by the $^{104}$Ru(t,p)$^{106}$Ru reaction.

[d] The $2^+ \to 0^+$ and $4^+ \to 2^+$ transition in $^{132}$Te and the $2^+ \to 0^+$ transition in $^{134}$Te were observed by Bergström et al.[11] following beta decay of fission products analyzed by an on-line mass separator.

[e] The decay of $^{134}$Te has also been reported by John et al.[12] who measured the $6^+ \to 4^+$, $4^+ \to 2^+$, and $2^+ \to 0^+$ transition in their study on delayed gamma-rays in $^{252}$Cf fission.

[f] The $2^+ \to 0^+$ transitions in $^{140}$Ba and $^{142}$Ba have been observed by Alväger et al.[13] following beta decay of mass separated fragments.

[g] The $2^+ \to 0^+$ transition in $^{144}$Ce has been observed by Wilhelmy et al.[14]

[h] The rotational band in $^{156}$Sm has been observed in the $^{154}$Sm(t,p)$^{156}$Sm reaction by Bjerrgaard et al.[15]
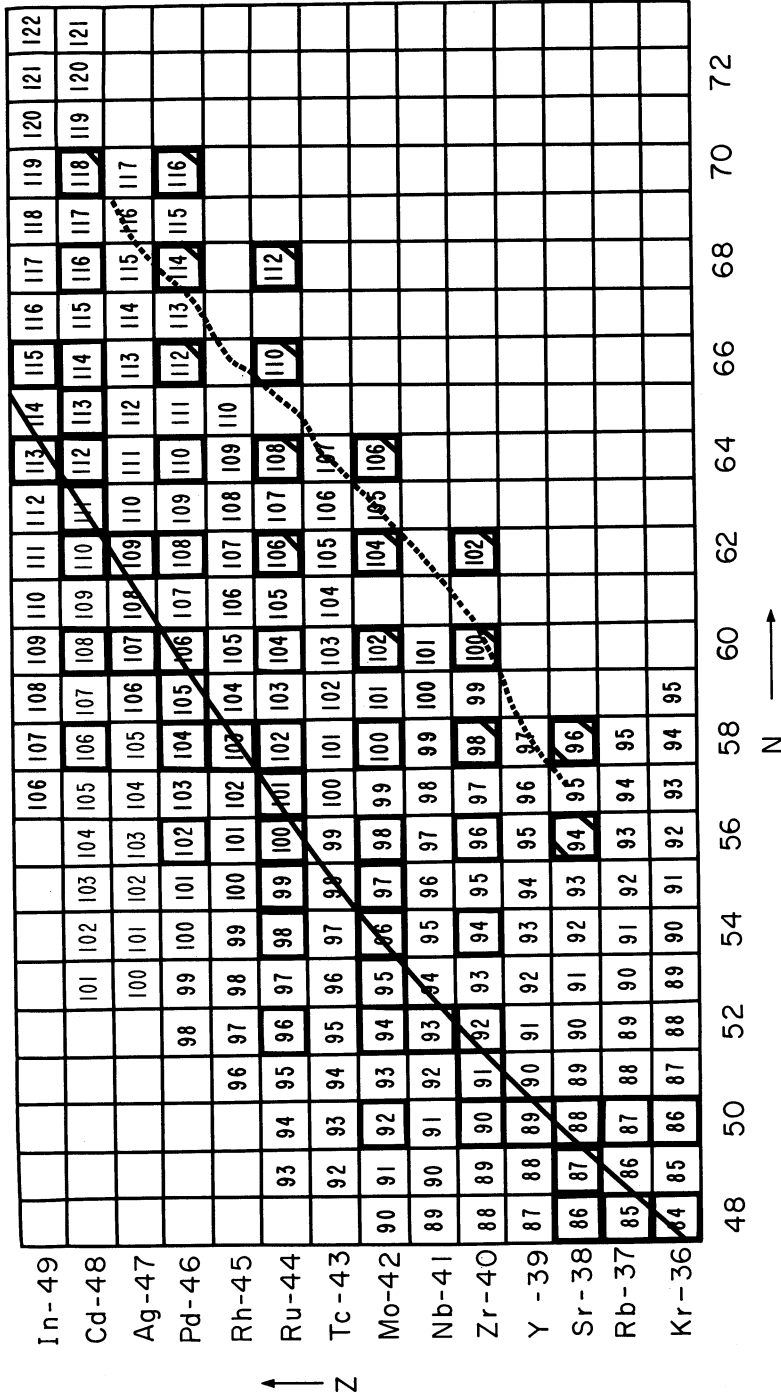
LIGHT FISSION FRAGMENT REGION

Fig. 1. A region of the chart of nuclides presenting the isotopes produced as light fission products. The solid line approximates the line of β stability and the heavy squares in this region are the beta stable isotopes. The dotted line represents the $Z_p$ values for the fission of $^{252}$Cf and the heavy squares with diagonal lines in the lower right hand corner are the even-even products observed in the current experiments. The heavy squares with an additional diagonal line in the upper corner are isotopes for which our assignments are tentative.

HEAVY FISSION FRAGMENT REGION
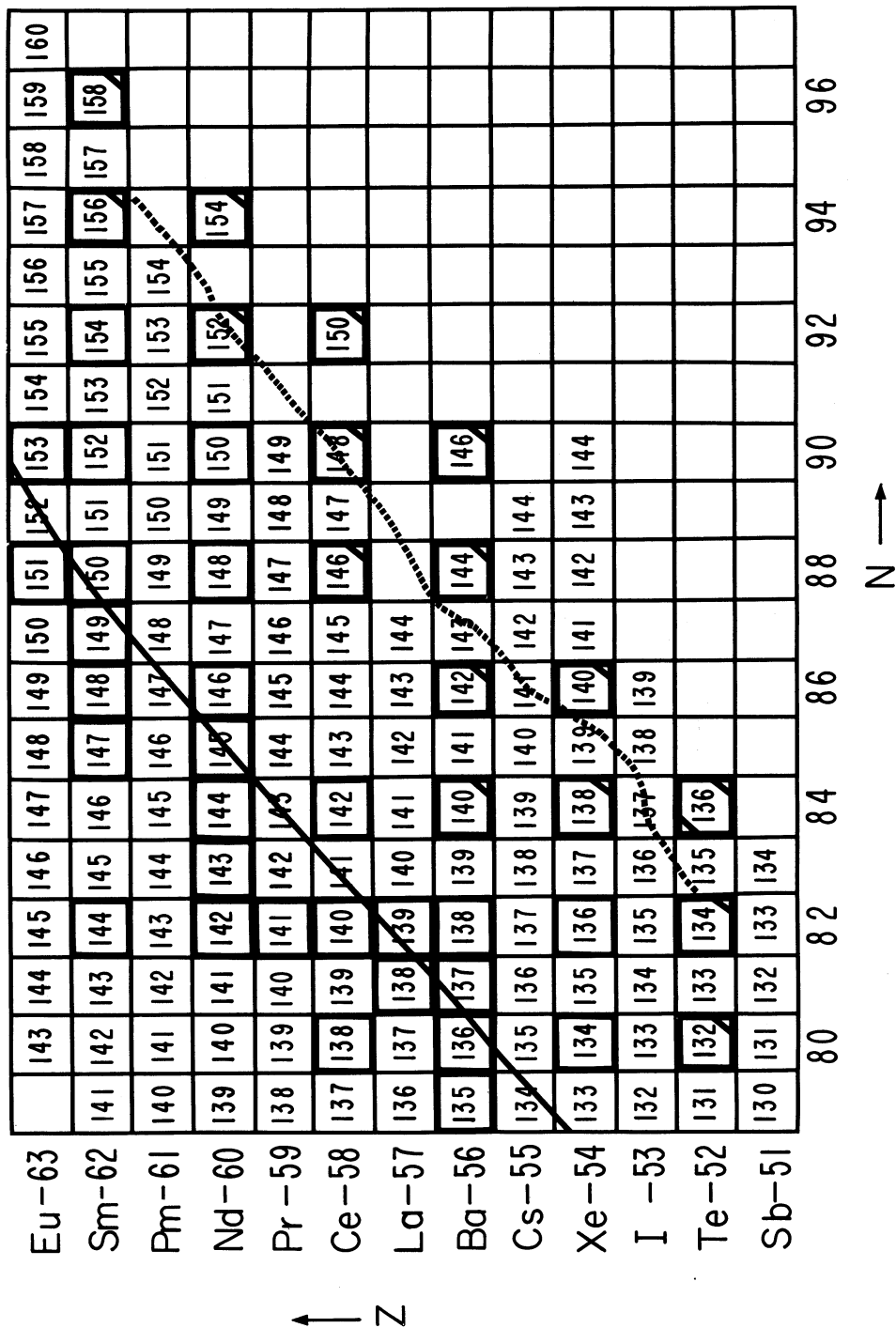
Fig. 2.  Same as Fig. 1 but presented for the heavy fission product region.
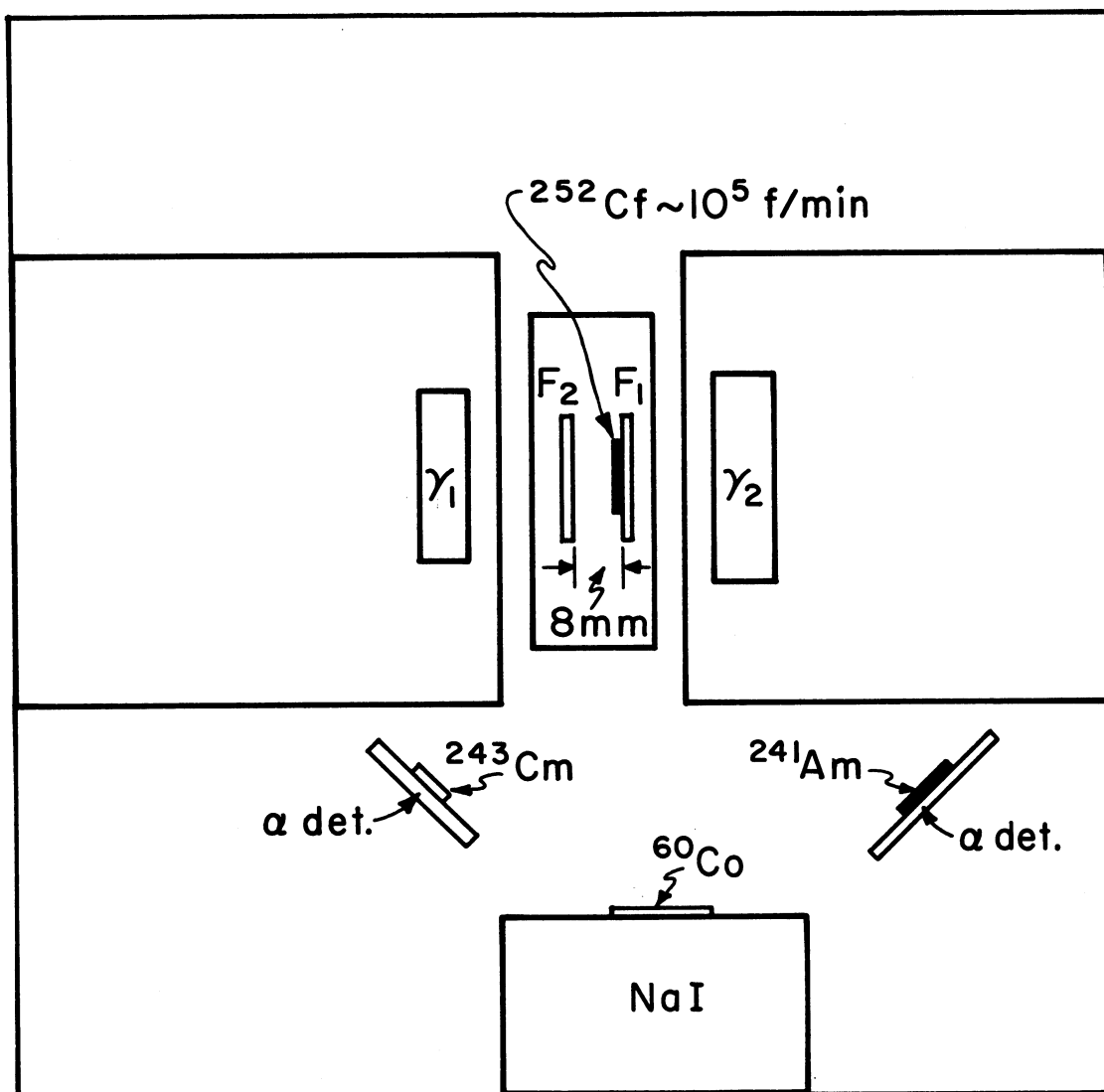
XBL703-2403

Fig. 3. Schematic representation of detector system. Detectors F1 (with elec-
trodeposited $^{252}$Cf) and F2 measured energies of fragments. Detectors $\gamma_1$
and $\gamma_2$ measured energies of $\gamma$-rays and/or x-rays. External sources for
stabilization of the photon detectors were $^{243}$Cm ($\alpha$-$\gamma$ coincidence), $^{60}$Co
($\gamma$ - $\gamma$ coincidence) and $^{241}$Am ($\alpha$ - $\gamma$ coincidence).
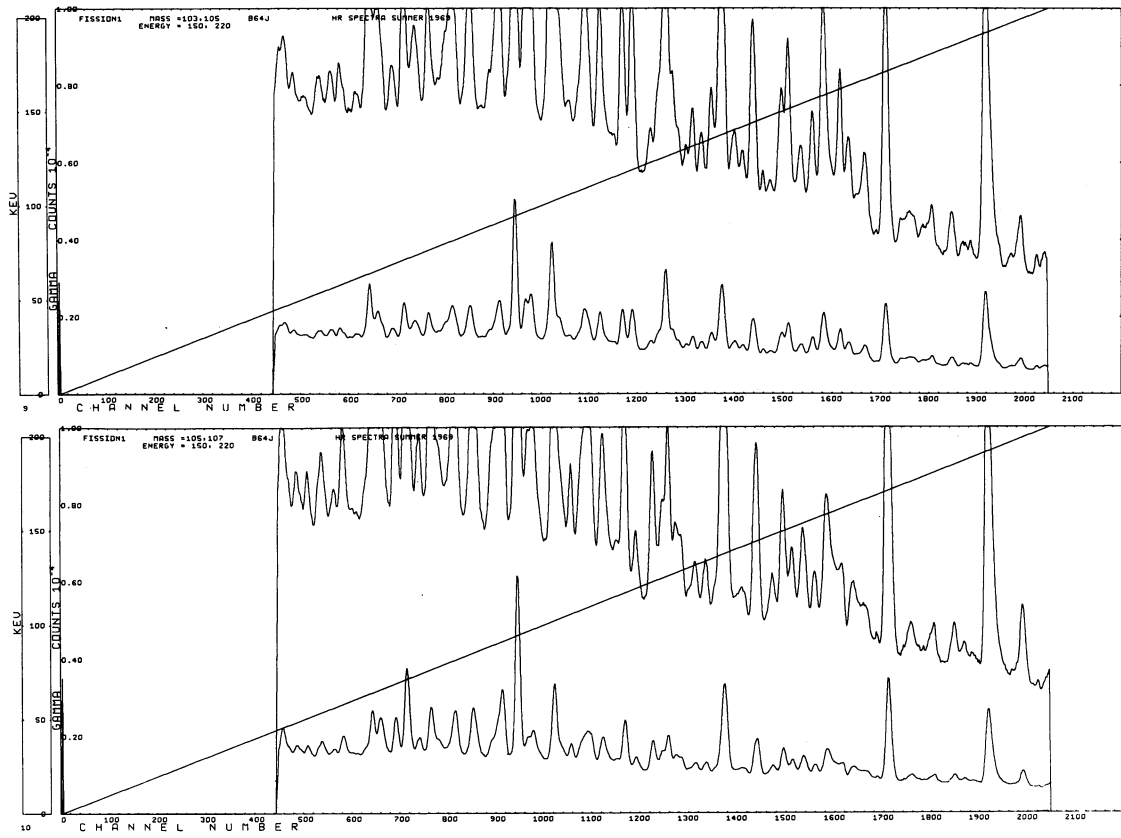
Fig. 4. Gamma ray spectra recorded using a 1 cm$^3$ high resolution Ge(Li) detector. Results shown are for fission fragments that were stopped in the plated detector having masses 103-105 and 105-107.
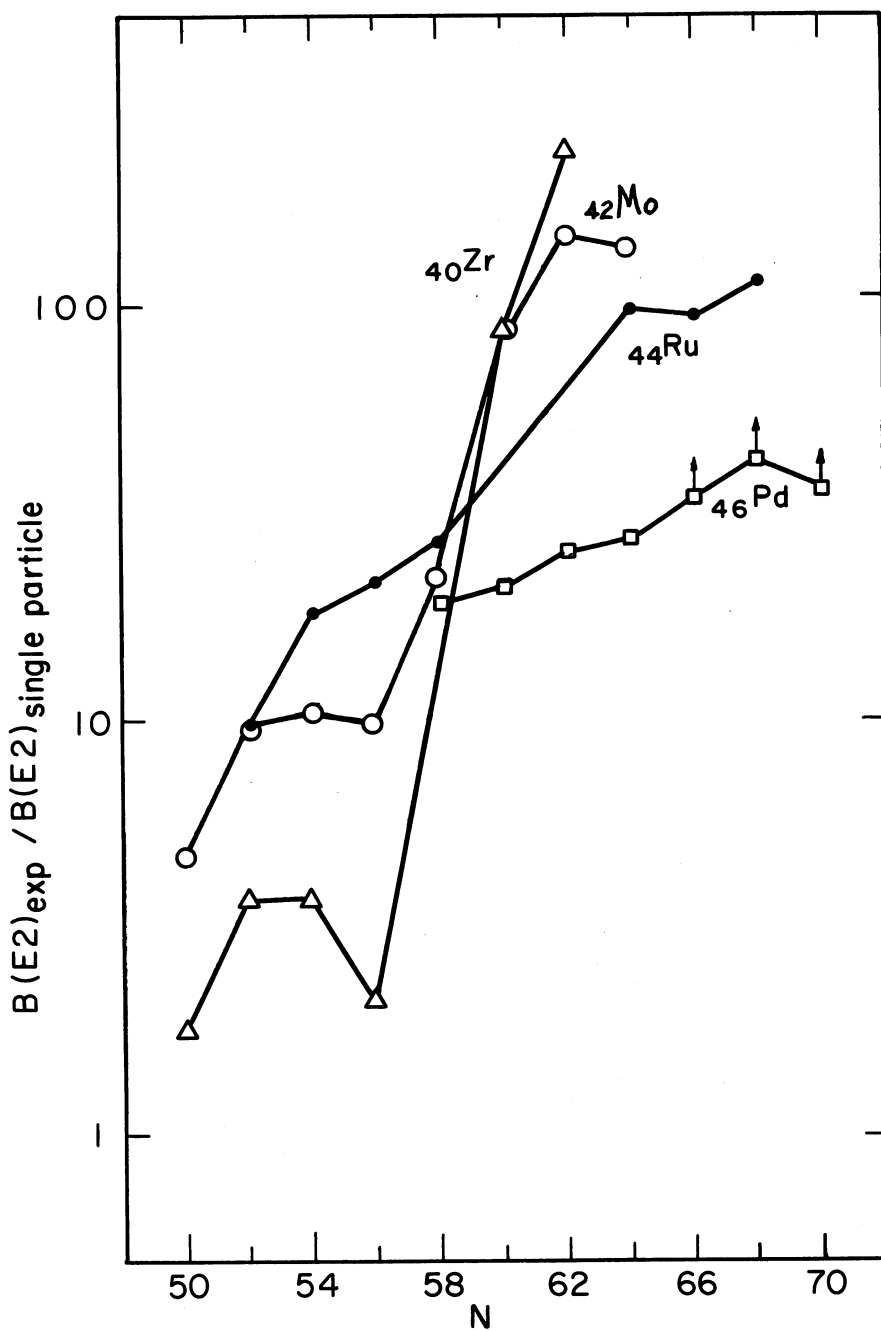
XBL 708-1785
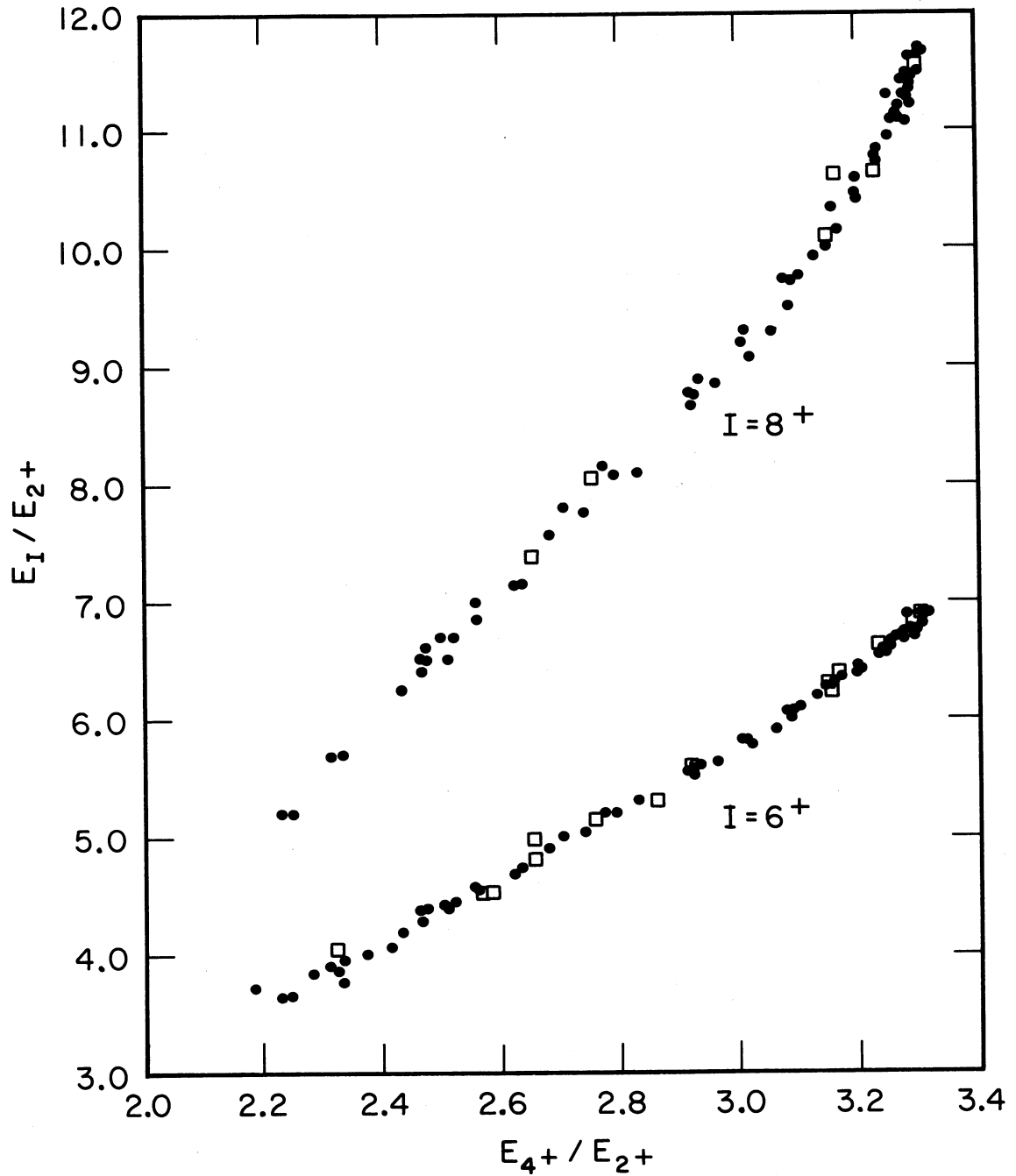
XBL 708 - 3630

Fig. 5. Plot of the energy ratios E8$^+$/E2$^+$ and E6$^+$/E2$^+$ versus E4$^+$/E2$^+$. The data presented as dots were taken from ref. 1 and those presented as open squares are the current experimental results.
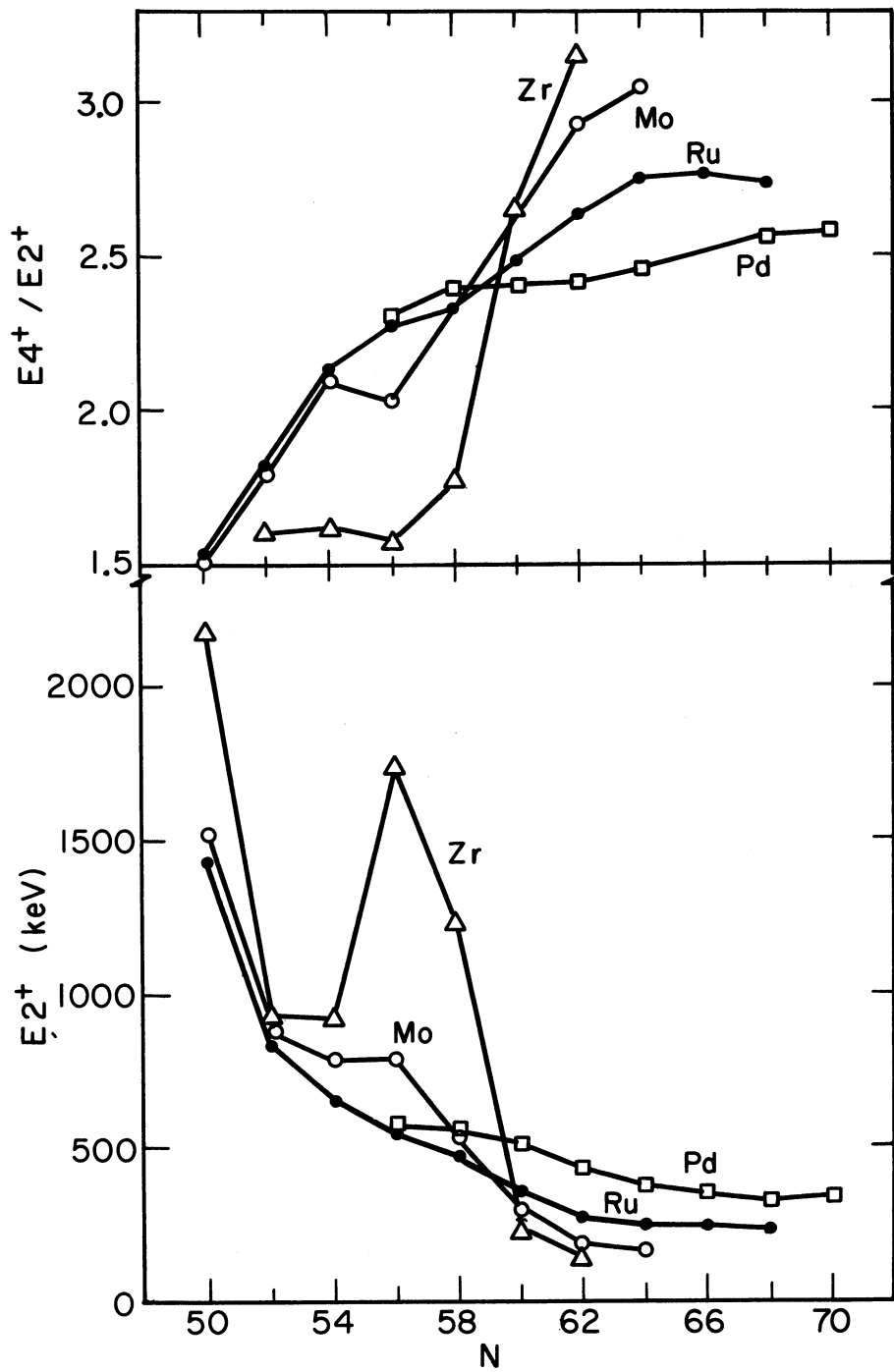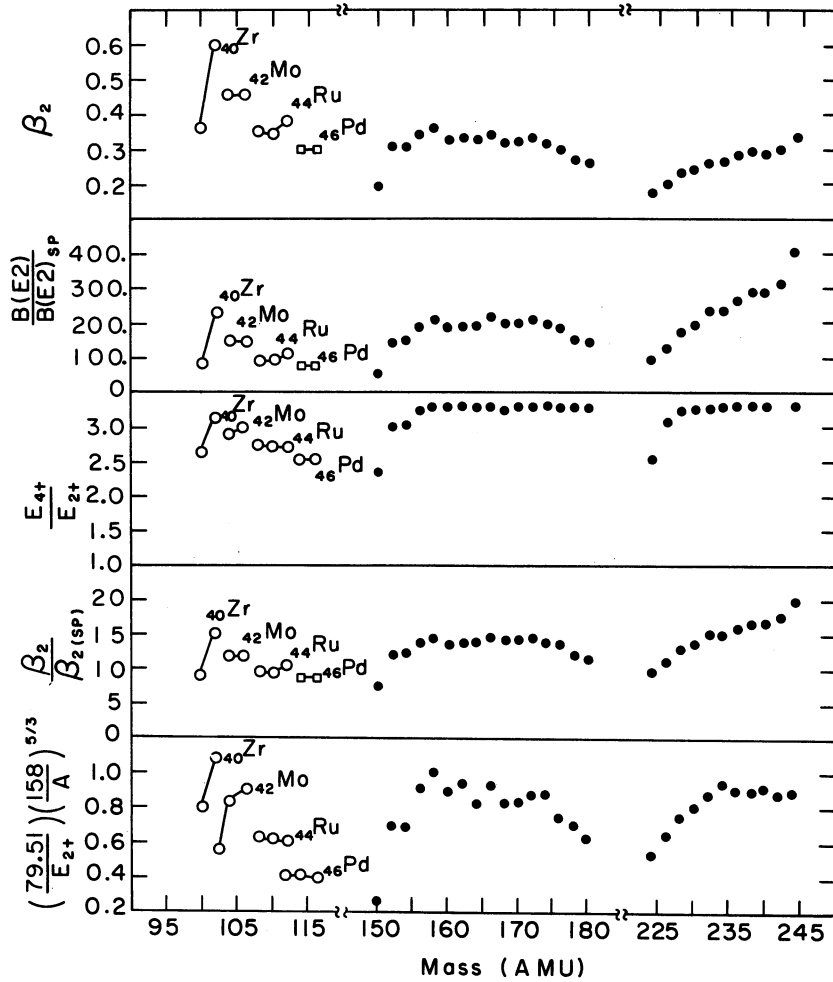
XBL704-2745

Fig. 6.  Energies of the lowest $2^+$ levels and $E4^+/E2^+$ energy ratios in the Zr - Pd region.

XBL704-2744

Fig. 7. B(E2)$_{exp}$/B(E2)$_{SP}$ in the Zr - Pd region. The data presented for the most neutron rich isotopes are from the current experimental results and the others are from ref. 17.

XBL705-2752

Fig. 8. A composite plot presenting five indicators of deformation plotted as a function of mass. The mass intervals used contain only the current light fission product experimental region and a representative sampling from the two major known regions of deformation. The values of $\beta_2$, $\beta_{2SP}$, $B(E2)$, and $B(E2)_{SP}$ were extracted from relationships presented in ref. 17; the indicator $(79.51/E_{2^+}) \times (158/A)^{5/3}$, gives a relative comparison between the energies of the first $2^+$ states on a basis which removes the inherent mass-dependence from the moment of inertia. The open circles represent current results obtained using experimental energies and life times. The open squares represent current results obtained using experimental energies and calculated life times (ref. 1). The closed circles represent literature values (refs. 1 and 17).
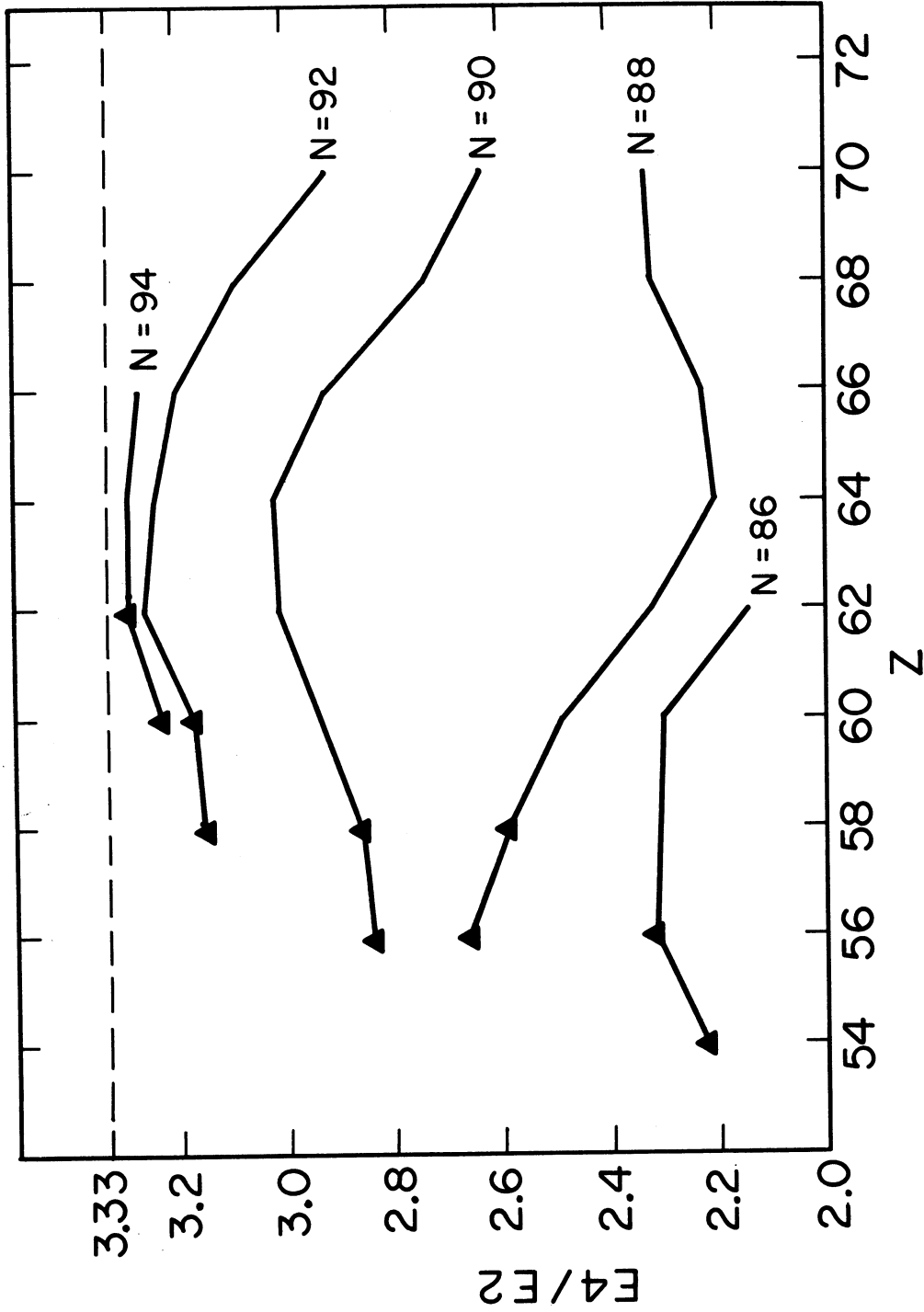
Fig. 9. Systematic behavior of the ratio E4/E2 as a function of proton number in the N = 86 - 92 region. Data presented as Δ are from the current experimental results and the other data are from refs. 22 and 23.

xBL706-3124